

BBAMEM 75134

## The effects of glycerol on the phase behaviour of hydrated distearoylphosphatidylethanolamine and its possible relation to the mode of action of cryoprotectants

W. Patrick Williams<sup>1</sup>, Peter J. Quinn<sup>1</sup>, Latchezar I. Tsonev<sup>2</sup>  
and Rumiana D. Koynova<sup>3</sup>

<sup>1</sup> Biomolecular Sciences Division, King's College London, London (U.K.), <sup>2</sup> Institute of Cryobiology and Freeze-drying, Sofia (Bulgaria)  
and <sup>3</sup> Central Laboratory of Biophysics, Bulgarian Academy of Sciences, Sofia (Bulgaria)

(Received 20 June 1990)

Key words: Glycerol; Phosphatidylethanolamine; Cryoprotectant; Phase behavior; Phase diagram

A phase diagram for 1,2-distearoylphosphatidylethanolamine (DSPE) dispersed in glycerol/water mixtures was constructed using data obtained from differential scanning calorimetry and time-resolved X-ray diffraction measurements. The phase sequence seen on heating the lipid remains the same for samples containing up to 70 wt% glycerol. Depending on the hydration conditions, the samples are either in a metastable lamellar gel ( $L_\beta$ ) or one or other of two possible sub-gel phases ( $L_c$  and  $L_{c'}$ ) at low temperatures. These phases convert first to a lamellar liquid crystalline ( $L_\alpha$ ) and then to an inverted hexagonal ( $H_{II}$ ) phase on heating. On cooling, the samples revert first to the  $L_\alpha$  and then to the  $L_\beta$  phase. Although the phase sequence is preserved, marked changes are seen in the transition temperatures between the different phases. The temperature of the transition between the  $L_\alpha$  and the  $H_{II}$  phases decreases strongly with increasing glycerol concentration while that of the  $L_c$  and  $L_{c'}$  phases to  $L_\alpha$ , and to a lesser extent that of the  $L_\beta$  to  $L_\alpha$  transition, increases. Substantial changes in phase behaviour are seen if the glycerol concentration is increased above 70 wt%. Under these conditions, the  $L_c$  and  $L_{c'}$  phases transform directly into the  $H_{II}$  phase on heating (a similar direct transition from the  $L_\beta$  to the  $H_{II}$  phase is seen above 80 wt% glycerol). An exothermic transition from the  $L_\beta$  phase to the  $L_{c'}$  phase is observed and there is also an increasing tendency for the samples to revert to the  $L_c$  or  $L_{c'}$  phases on storage. These changes in relative stability of the different phases are discussed in terms of a possible membrane Hofmeister effect and their relevance to the mode of action of cryoprotectants is explored.

### Introduction

Phosphatidylethanolamines are one of the major classes of phospholipids present in biological membranes. Their phase behaviour is known to be strongly influenced by such physiologically important parameters as temperature, pH, ionic strength and extent of hydration [1,2]. Phase separation of non-bilayer forming

lipids such as phosphatidylethanolamines has been suggested to play a major part in the development of lesions in membranes exposed to low temperatures [3–5]. This in turn, has led to interest in their interactions with cryoprotectants such as sugars, sugar alcohols and polyols. Recent studies have demonstrated that disaccharides [6,7], sugar alcohols and polyols [6] all promote the formation of the non-bilayer inverted hexagonal phase ( $H_{II}$ ) at the expense of the lamellar liquid-crystalline phase ( $L_\alpha$ ).

Five different phases have been characterised in aqueous dispersions of the longer chain phosphatidylethanolamines [8–10]. Two crystalline subgel phases ( $L_c$  and  $L_{c'}$ ) and a metastable gel phase ( $L_\beta$ ) have been identified. These three phases, which are all lamellar, melt to form a lamellar  $L_\alpha$  phase on heating. The non-bilayer  $H_{II}$  phase is formed at higher temperatures. The crystalline phases are normally formed by hydra-

Abbreviations: DLPE, DMPE, DPPE, DSPE and DAPE, 1,2-dilauryl-, 1,2-dimyristoyl-, 1,2-dipalmitoyl-, 1,2-distearoyl- and 1,2-diarachidonyl-phosphatidylethanolamine; DPPC, 1,2-dipalmitoylphosphatidylcholine;  $L_\alpha$ , liquid-crystal lamellar phase;  $L_\beta$ , gel lamellar phase;  $L_c$  and  $L_{c'}$ , crystal (sub-gel) lamellar phases;  $H_{II}$ , inverted hexagonal phase.

Correspondence: W.P. Williams, Biomolecular Sciences Division, King's College London, Campden Hill, London W8 7AH, U.K.

tion at temperatures below that of the gel to liquid-crystal transition.

Seddon et al. [10] have characterised two crystalline subgel phases for the shorter chainlength lipid DLPE which they refer to as the  $B_1$  and  $B_2$  forms. In the  $B_2$  form, the hydrocarbon chains of the lipids are packed on an orthorhombic lattice with their main axis perpendicular to the plane of the bilayer. The structural organisation of the  $B_1$  form is more problematic. The lipid chains are tilted at an angle of about  $40^\circ$  to the normal to the bilayer but the precise packing lattice still remains to be established. The  $L_c$  form of the longer chain ( $C_{16}$ – $C_{18}$ ) phosphatidylethanolamines appears to be directly analogous to the  $B_2$  form of DLPE [2,9]. Seddon et al. [2] have reported the existence of a tilted crystalline form in weakly hydrated DAPE that appears to correspond to the  $B_1$  form of DLPE which they designate as  $L_c'$ . Tenchov et al. [8] have also identified a second subgel form for racemic DPPE.

In this paper, we report the results of a combined calorimetric and X-ray diffraction study of the effects of glycerol on the phase behaviour of hydrated DSPE. A phase diagram illustrating the effects of glycerol/water mixtures on the behaviour of DSPE is presented. The low-temperature crystalline subgel phases ( $L_c$  and  $L_c'$ ), are identified and characterised. The presence of glycerol is shown to stabilise the non-bilayer  $H_{II}$  phase, and to a lesser extent the metastable gel-phase  $L_\beta$ , at the expense of the liquid-crystal  $L_\alpha$  phase and to stabilise the crystal phases at the expense of the  $L_\beta$  phase. The mechanisms underlying these changes in phase stability are discussed in terms of their possible relevance to the mode of action of cryoprotectants.

## Materials and Methods

Synthetic 1-DSPE was purchased from Avanti (Pelham, AL, U.S.A.) and glycerol from Fluka (Switzerland). TLC and gas chromatography measurements indicated that the lipid was at least 99% pure.

Appropriate amounts of lipid in glycerol/quartz bi-distilled water mixtures containing 0, 25, 50, 60, 70, 80 and 100 wt% glycerol were either equilibrated at  $60^\circ\text{C}$  for 30 min or subjected to repeated freeze-thaw cycles. The samples were vortex-mixed several times during preparation. The final water content of the mixtures was checked by refractive index measurements using an Abbe refractometer.

Thermograms were recorded at a heating rate of  $0.5^\circ\text{C min}^{-1}$  using a Privalov differential adiabatic scanning calorimeter, DASM-1M. The lipid concentration for all the samples was 0.03 wt% lipid. Control measurements were carried out using a DuPont 1090 Thermo-analyzer, for which both the lipid concentration (25 wt%) and the scan rate ( $2^\circ\text{C}$  or  $5^\circ\text{C}$  per min) were similar to those used in the X-ray studies. The transition

temperatures and enthalpy values obtained using the two instruments were in good agreement.

Aliquots taken from a sample of DSPE dispersed in 70 wt% glycerol cycled between 40 and  $110^\circ\text{C}$  at a heating/cooling rate of  $5^\circ\text{C min}^{-1}$  for 3 hours were analysed by TLC to test for possible lipid degradation. Samples were run on silica gel 60 plates using chloroform/methanol/glacial acetic acid/water (25:15:4:2, by vol.) and hexane/diethyl ether/glacial acetic acid (60:40:2, by vol.) to separate lyso-lipids and fatty acids, respectively. The plates were developed by spraying with 2,7-dichlorofluorescein (0.2% w/v in methanol) and viewed under UV light. Limited lipid hydrolysis was observed to have occurred but was estimated to be less than 5%.

Real-time X-ray diffraction measurements were performed using a monochromatic (0.15 nm) X-ray beam at station 8.2 of the Daresbury Synchrotron Radiation Source as previously described [8]. The samples, which contained 25% lipid, were prepared by equilibration at  $60^\circ\text{C}$  as described above. Temperature scans were carried out using a modified Linkam (Tadworth, U.K.) temperature-controlled microscope stage.

## Results

### *Aqueous dispersions of DSPE*

Typical thermograms for DSPE dispersed in glycerol-free water are presented in Fig. 1. The thermal behaviour of the samples depends on their thermal history. Samples hydrated at  $60^\circ\text{C}$  are characterised in their first heating cycle by a large endotherm, with a  $T_m$  of  $75^\circ\text{C}$  and an enthalpy of  $16.8\text{ kcal mol}^{-1}$ , and a second much smaller endotherm with a  $T_m$  of  $101^\circ\text{C}$  and enthalpy of  $0.62\text{ kcal mol}^{-1}$ . The lower temperature endotherm is replaced in subsequent scans by an endotherm with a  $T_m$  of  $74^\circ\text{C}$  and an enthalpy of  $8.6\text{ kcal mol}^{-1}$ . The smaller, high temperature endotherm remains unchanged apart from a slight reduction in cooperativity. Samples hydrated at  $80^\circ\text{C}$  (i.e. in the liquid-crystal state) showed this latter pattern of behaviour even for the initial heating scan.

This pattern of behaviour is well documented for saturated phosphatidylethanolamines [10–13]. It has been shown to reflect the presence of a subgel crystalline phase of the lipid on initial hydration at temperatures below that of the transition to the liquid-crystal state. Samples hydrated at temperatures above this transition normally show no sign of subgel formation. On this basis, the endotherm at  $75^\circ\text{C}$  corresponds to a transition between one of the subgel crystalline phases and the  $L_\alpha$  phase and that at  $74^\circ\text{C}$  to a transition between the  $L_\beta$  and  $L_\alpha$  phases. No evidence of restoration of the initial subgel phase was seen in DSPE samples stored for four days at  $20^\circ\text{C}$ . Restoration of the subgel phase following high-temperature treatment

has been shown to take place after 10 and 20 days of low-temperature storage for the shorter chain phosphatidylethanolamines, DLPE and DMPE, respectively [13], and it is conceivable that long-term storage of hydrated DSPE may lead to a similar restoration.

The particular subgel phase adopted by samples hydrated below the melting transition, is dependent on the hydration conditions. Samples subjected to prolonged hydration at 60°C give rise to the  $L_c$  form reported to occur in DSPE dispersions containing limited water. Samples hydrated at 60°C for short times, or subjected to freeze-thaw cycles, in contrast, give rise to the  $L_c$  form reported by Seddon et al. [2].

Time-resolved X-ray measurements illustrating the conversion of a DSPE sample from the  $L_c$  to the  $L_\alpha$  phase on first heating are presented in Fig. 2a. Corresponding measurements on the same sample illustrating its conversion from  $L_\beta$  to the  $L_\alpha$  phase on cooling and reheating are presented in Fig. 2b. The differences in the diffraction patterns of the low-temperature phase prior to first melting and after heat-treatment are quite clear. In both cases, the transition to the  $L_\alpha$  phase

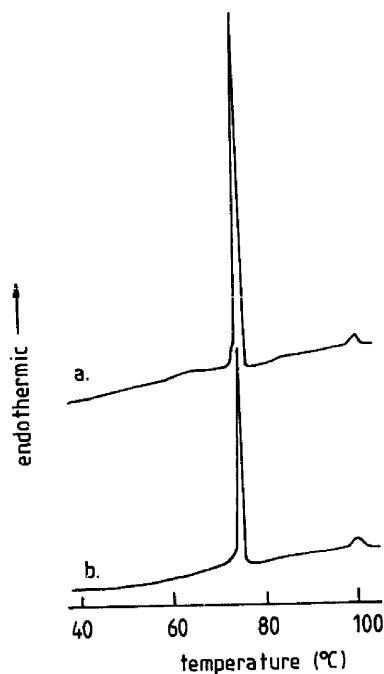


Fig. 1. Differential scanning calorimetric heating thermograms of DSPE dispersed in excess water. Sample preparation was carried out at 60°C (i.e., below the gel-to-liquid crystal phase transition temperature). Scan (a) initial heating thermogram of sample pre-equilibrated at 20°C for three days. Scan (b) second heating thermogram recorded immediately after cooling from 105°C to 40°C. Scanning rates were 0.5°C min<sup>-1</sup>.

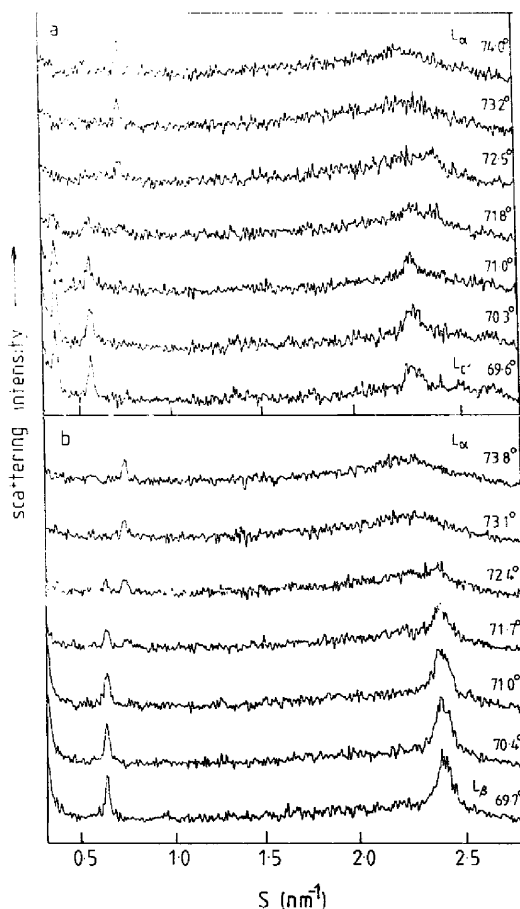


Fig. 2. Time resolved X-ray scattering intensity versus reciprocal spacing as a function of temperature for samples of DSPE in water hydrated at 60°C during (a) first heating and (b) second heating immediately after cooling to 60°C. The heating rates were 2°C min<sup>-1</sup>. The individual traces were obtained by averaging ten frames of acquisition time of 1.5 s per frame.

occurs at about 72–73°C, close to the value obtained in the calorimetry studies. Samples initially hydrated in the liquid-crystal state showed no trace of the subgel pattern seen in Fig. 2a.

More detailed static X-ray patterns for the two subgel phases  $L_c$  and  $L_c'$  are presented, together with the corresponding patterns for the  $L_\beta$ ,  $L_\alpha$  and  $H_{II}$  phases of hydrated DSPE, in Figs. 3a–3e. The diffraction patterns for the two subgel phases and the  $H_{II}$  phases are for samples containing glycerol, which tend to show rather more ordered diffraction patterns than the glycerol-free samples, but the basic patterns are the same.

The wide-angle region of the  $L_c$  phase (Fig. 3a) is characterised by the presence of two sharp diffraction

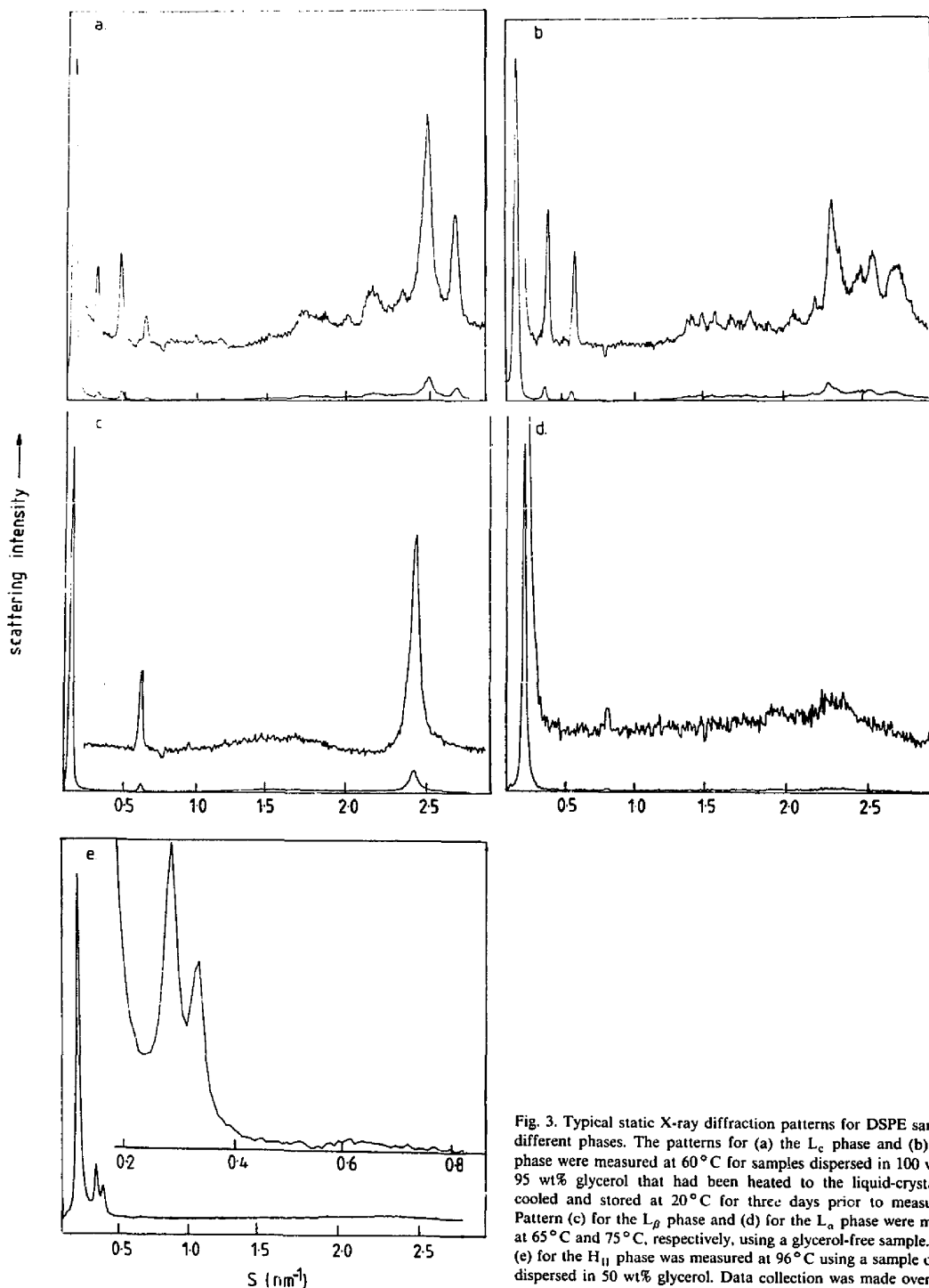


Fig. 3. Typical static X-ray diffraction patterns for DSPE samples in different phases. The patterns for (a) the  $L_c$  phase and (b) the  $L_c$  phase were measured at  $60^\circ\text{C}$  for samples dispersed in 100 wt% and 95 wt% glycerol that had been heated to the liquid-crystal state, cooled and stored at  $20^\circ\text{C}$  for three days prior to measurement. Pattern (c) for the  $L_\beta$  phase and (d) for the  $L_\alpha$  phase were measured at  $65^\circ\text{C}$  and  $75^\circ\text{C}$ , respectively, using a glycerol-free sample. Pattern (e) for the  $H_{II}$  phase was measured at  $96^\circ\text{C}$  using a sample of DSPE dispersed in 50 wt% glycerol. Data collection was made over 15 s in each case.

bands with spacings of 0.370 and 0.395 nm and two less prominent diffraction maxima centered at about 0.46 and 0.58 nm. These wide-angle spacings are in good agreement with the values of 0.376, 0.400, 0.452 and 0.587 nm reported by Seddon et al. [10] for the  $B_2$  form of DLPE and the values of 0.360, 0.390, 0.470 and 0.582 reported by Tenchov et al. [9] for the  $L_c$  form of L-DPPE. The lamellar repeat distance is 6.1 nm. In good agreement with the value of 6.0 nm reported for DSPE by Seddon et al. [2]. The diffraction pattern for the  $L_c$  phase (Fig. 3b) is characterised by a lamellar repeat distance of 5.25 nm, a prominent wide-angle diffraction maximum at 0.437 and two less prominent maxima at 0.393 and 0.372 nm. The reduced lamellar repeat distance suggests that the hydrocarbon chains are tilted with respect to the normal to the plane of the lamellae in a manner analogous to that reported by Seddon et al. [10] for the  $B_1$  form of DLPE. The positions of the wide-angle bands are, however, significantly different indicating that the chain packing differs from that in DLPE.

On heating, the samples are first converted to a lamellar liquid-crystal phase,  $L_\alpha$ , with a lamellar spacing of about 5.3 nm and a diffuse wide angle maximum centered at about 0.44 nm (Fig. 3d). At higher temperatures, the samples are converted to a  $H_{II}$  phase characterised by low angle spacings indexing in the series  $d : d/\sqrt{3} : d/\sqrt{4} : d/\sqrt{7}$  (Fig. 3e). Samples hydrated in, or cycled through, the liquid-crystal state are characterised by a lamellar repeat distance of 6.25 nm and have a single sharp wide angle spacing of 0.41 nm diagnostic of a conventional  $L_\beta$  gel phase [14] (Fig. 3c). The lamellar repeat distance is again in good agreement with the value of 6.3 nm reported by Seddon et al. [2] for the  $L_\beta$  phase of DSPE.

Thermograms for DSPE samples dispersed in aqueous glycerol solutions containing less than 70 wt% glycerol are broadly similar to those seen for samples dispersed in water apart from marked decreases in the  $T_m$  value of their  $L_\alpha$ - $H_{II}$  transitions and rather less marked increases in the  $T_m$  values of their subgel to  $L_\alpha$  transitions. Time-resolved X-ray data confirm that the phase sequences in these dispersions are identical to those in aqueous dispersions.

The thermal behaviour of samples dispersed in higher glycerol concentrations is much more complex. Typical thermograms for samples dispersed in 70 and 100 wt% glycerol are presented in Figs. 4 and 5, respectively. During the first heating scan a single large endotherm reflecting a direct transformation of the  $L_c$  phase into the  $H_{II}$  phase is observed as in samples dispersed in low glycerol concentrations.

The thermograms for subsequent heating scans are more complex. The main features of such thermograms obtained following cooling to room temperature are the presence of two endotherms and an exotherm. Exam-

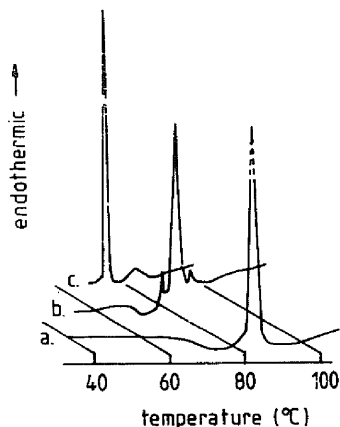


Fig. 4. Differential scanning calorimetric heating thermograms of DSPE dispersed in excess 70 wt% glycerol. Scan (a) initial heating thermogram, scan (b) second heating thermogram recorded after equilibration at 20°C for 40 h, scan (c) third heating scan immediately after cooling from 105°C to 70°C. The sample was initially dispersed at 60°C and heating rates were 0.5°C min<sup>-1</sup>.

ples of these can be seen in Figs. 4b, 5b and 5c. X-ray measurements indicate that the lower temperature endotherm corresponds to a  $L_\beta$ - $H_{II}$  transition and the higher temperature endotherm to a  $L_c$ - $H_{II}$  transitions.

The relative size of the two endotherms depends strongly on the concentration of glycerol and the thermal history of the samples. Under normal conditions all samples initially form the  $L_\beta$  phase on cooling. If the samples are reheated immediately after cooling to 70°C,

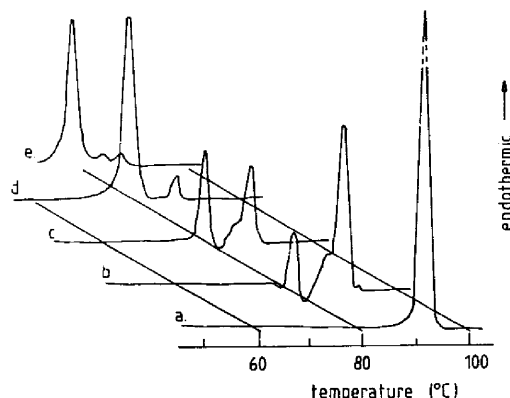


Fig. 5. Differential scanning calorimetric heating thermograms of DSPE dispersed in excess glycerol. Scan (a) initial heating thermogram, scan (b) second heating thermogram recorded after equilibration at 20°C for 15 h, scan (c) third heating scan immediately after cooling from 105°C to 50°C, scan (d) fourth heating immediately after cooling from 105°C to 50°C, scan (e) fifth heating immediately after cooling from 105°C to 70°C. The sample was initially dispersed at 60°C and heating rates were 0.5°C min<sup>-1</sup>.

the higher-temperature endotherm corresponding to the  $L_c$ - $H_{II}$  transition is virtually eliminated and the lower-temperature  $L_\beta$ - $H_{II}$  endotherm dominates the thermogram as illustrated in Figs. 4c and 5e. Conversion of the  $L_\beta$  phase to  $L_{c'}$ , which is signalled by the exotherm centered between about  $60^\circ\text{C}$  and  $70^\circ\text{C}$ , requires a period of incubation at temperatures below  $70^\circ\text{C}$ . A direct demonstration of the formation of  $L_{c'}$  from  $L_\beta$ , which is facilitated by increasing glycerol concentrations, is provided in the time-resolved X-ray diffraction patterns for DSPE dispersed in 90 wt% glycerol presented in Fig. 6.

In our experience, heated samples stored at room temperature for several days relax from the  $L_\beta$  to the  $L_{c'}$  or the  $L_c$  phase. The factors governing which phase is formed are still obscure. Occasionally, at very high glycerol concentrations, the subgel phase will form directly from, and co-exist with, the  $H_{II}$  phase. This is illustrated in the time-resolved X-ray diffraction patterns for DSPE dispersed in 100 wt% glycerol presented in Fig. 7. The sample, which was cooled from  $90^\circ\text{C}$  at a rate of  $6^\circ\text{C min}^{-1}$ , was initially in the  $H_{II}$  state. As it cooled, it slowly converted to the  $L_{c'}$  state. This conver-

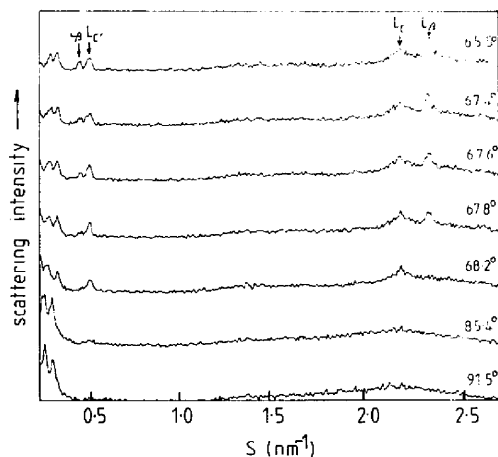


Fig. 7. Selected frames illustrating changes in X-ray scattering intensity as a function of reciprocal lattice spacing for a sample of DSPE in excess glycerol cooled from  $91.5^\circ\text{C}$  to  $65^\circ\text{C}$  at a rate of  $5^\circ\text{C min}^{-1}$ . The data acquisition time for each frame was 1.5 s. The temperatures at which the individual frames were recorded are indicated.

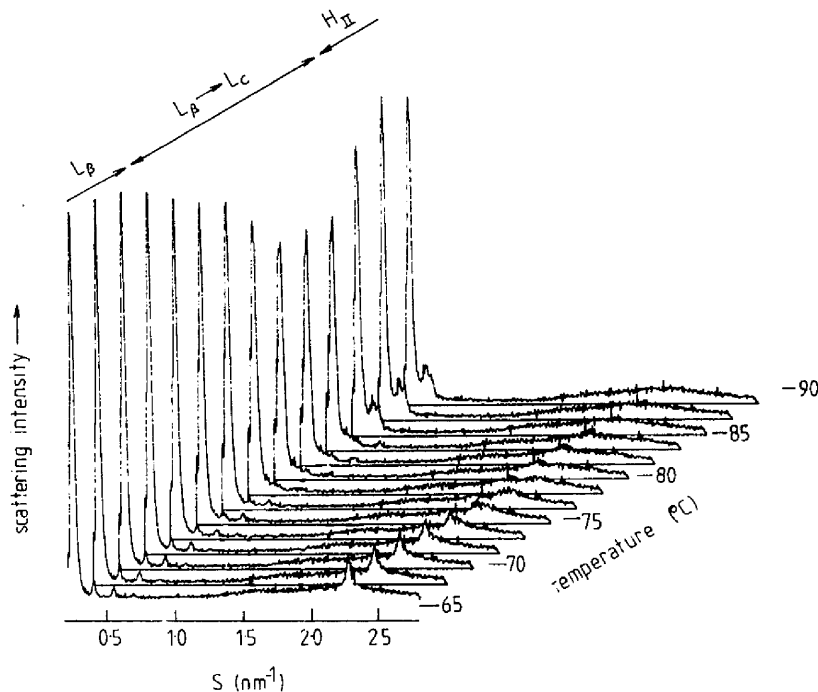


Fig. 6. Time-resolved X-ray diffraction measurements made using a sample of DSPE in 90 wt% glycerol cooled to  $60^\circ\text{C}$  and immediately re-heated at a rate of  $5^\circ\text{C min}^{-1}$ . Data collection was for 1.5 s per frame and only every fifteenth frame of the total data set is shown.

sion was signalled by the appearance of the second and third order diffraction peaks of the  $L_c$  phase, which started at about 85°C. Formation of  $L_c$  continued until the remainder of the sample abruptly converted from  $H_{II}$  to the  $L_\beta$  phase at about 68°C. A similar co-existence of the  $L_c$  and  $H_{II}$  phases has been reported in partially hydrated dispersions of DAPC [2]. The peaks corresponding to the  $L_\beta$  phase disappeared at about 80°C on reheating, while those corresponding to  $L_c$  persisted until the sample reached about 90°C. The transition temperatures in the heating cycle are thus close to those predicted by calorimetry.

A diagram illustrating the phase relationships of DSPE dispersed in glycerol/water mixtures is shown in Fig. 8. A summary of the  $T_m$  values for the transitions between the different phases, together with the corresponding molar enthalpy values, is provided in Tables I and II. The data presented in Fig. 8 relates to samples initially hydrated in the gel state. It must be emphasized that the particular subgel form obtained on initial hydration is dependent on the method of sample preparation adopted and that both the  $L_c$  and  $L_c'$  forms can be formed on initial hydration at all glycerol concentrations.

Seddon et al. [2] have shown that the low-angle spacings of the different hydrated phases of DSPE in dispersions containing limited amounts of water show varying dependencies on water content. Corresponding measurements for DSPE in glycerol/water mixtures are presented in Fig. 9. The pattern of behaviour is very similar. The spacing for the  $H_{II}$  phase decreases sharply as the glycerol content is increased and the water content is decreased. The spacings for the  $L_\alpha$  and  $L_\beta$  phases show much less marked dependencies on water content and the spacings for the two subgel phases are independent of the water content of the dispersing medium.

The major difference between the changes in the low-angle spacings with increasing glycerol content ob-

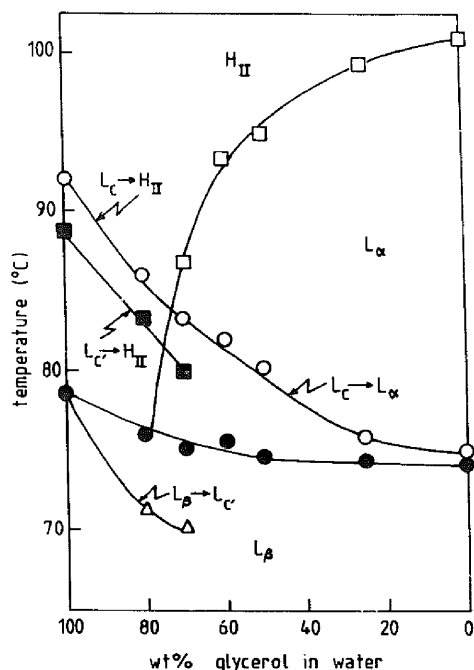


Fig. 8. Phase diagram illustrating the behaviour of DSPE dispersed in excess glycerol/water mixtures. The  $T_m$  values for the  $L_c$ - $L_\alpha$  (or  $H_{II}$ ) ( $\circ$ ) and the  $L_\alpha$ - $H_{II}$  ( $\square$ ) transitions were obtained from initial heating scans of samples hydrated in the gel state. The corresponding values for the  $L_\beta$ - $L_\alpha$  (or  $H_{II}$ ) ( $\bullet$ ) transitions were obtained from scans of the same samples reheated directly after cooling to 70°C. The  $T_m$  values for the  $L_\beta$ - $L_c$  ( $\Delta$ ) and the  $L_c$ - $H_{II}$  transitions ( $\blacksquare$ ) were estimated from the positions of the corresponding exotherms and endotherms of samples that had been cooled to lower temperatures.

served in the present study and those for dispersions with decreasing water activities, is the sharp decrease in the low-angle spacing for the  $L_\beta$  phase that occurs on

TABLE I

Transition temperatures ( $T_m$ ) and molar enthalpy values ( $\Delta H$ ) for DSPE dispersed in glycerol/water mixtures

Glycerol wt%	$L_c \rightarrow L_\alpha$ ( $H_{II}$ ) <sup>a,b</sup>		$L_\alpha \rightarrow H_{II}$		$L_\beta \rightarrow L$ ( $H_{II}$ ) <sup>a,c</sup>	
	$T_m$ (°C)	$\Delta H$ (kcal mol <sup>-1</sup> )	$T_m$ (°C)	$\Delta H$ (kcal mol <sup>-1</sup> )	$T_m$ (°C)	$\Delta H$ (kcal mol <sup>-1</sup> )
0	75	16.8	100.8	0.62	74.1	9.6
25	75.9	14.8	99.2	0.83	74.4	8.1
50	80.1	17.5	94.8	0.58	74.7	6.7
60	81.9	17.6	93.3	0.72	75.6	7.2
70	83.2	14.3	—	—	75.1	7.2
80	86.1	17.4	—	—	76.1	6.2
100	91.6	16.8	—	—	78.7	4.1

<sup>a</sup> Samples dispersed in 80–100 wt% glycerol pass from the gel state directly to  $H_{II}$ .

<sup>b</sup> Values taken from first heating curve of samples hydrated in the gel state.

<sup>c</sup> Values taken from heating curves of samples cooled from the liquid-crystal state and reheated immediately.

TABLE II

Transition temperatures ( $T_m$ ) and molar enthalpy values for transitions involving  $L_c$  phase

Glycerol wt%	$L_\beta \rightarrow L_c$ <sup>a</sup>		$L_c \rightarrow H_{II}$ <sup>b</sup>	
	$T_m$ (0°C)	$\Delta H$ (kcal mol <sup>-1</sup> )	$T_m$ (0°C)	$\Delta H$ (kcal mol <sup>-1</sup> )
70	70.0	-1.4	77.7	7.3
80	72.2	-1.9	83.2	10.4
100	80.0	-	87.5	10.2

<sup>a</sup> Exothermic transition.

<sup>b</sup> Calculated according to the formula  $\Delta h_1/(1 - \Delta h_2/\Delta h)$ , where  $\Delta h_1$  and  $\Delta h_2$  are the molar enthalpies calculated from the  $L_\beta \rightarrow H_{II}$  and  $L_c \rightarrow H_{II}$  endotherms of samples reheated after cooling below 70°C and  $\Delta h$  is the value for the  $L_\beta \rightarrow H_{II}$  endotherm of samples reheated immediately after cooling to 70°C.

increasing the glycerol content of the dispersing medium above about 70 wt%. This decrease coincides with the point at which the samples pass directly from the  $H_{II}$  phase to the  $L_\beta$  phase on cooling without the intervention of an  $L_\alpha$  phase. It could, in principle, correspond to a decrease in the thickness of the solvent layer between adjacent lipid bilayers, a tilting of the lipid chains or a combination of these two effects.

A similar sharp decrease in the lamellar repeat period has been reported by McDaniel et al. [15] for DPPC dispersions in glycerol/water mixtures, again at about 70 wt% glycerol. In this case, analysis of electron density profiles showed that the decrease was the result of both a sharp drop in bilayer thickness and a continuous

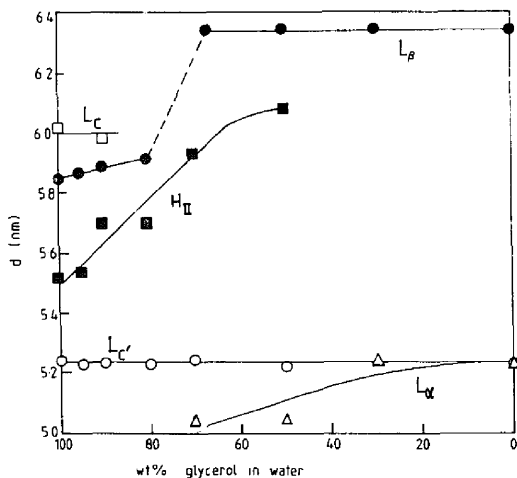


Fig. 9. Plot illustrating the dependence of the low angle spacings of  $L_\alpha$  ( $\Delta$ ),  $L_\beta$  ( $\bullet$ ),  $L_c$  ( $\square$ ),  $L_c'$  ( $\circ$ ) and  $H_{II}$  ( $\blacksquare$ ) spacings on glycerol concentration. Measurements for  $L_\beta$ ,  $L_c$ , and  $L_c'$  phases were performed at 65°C. The measurements for the  $L_\alpha$  and  $H_{II}$  phases were recorded at 75° and 90°C, respectively.

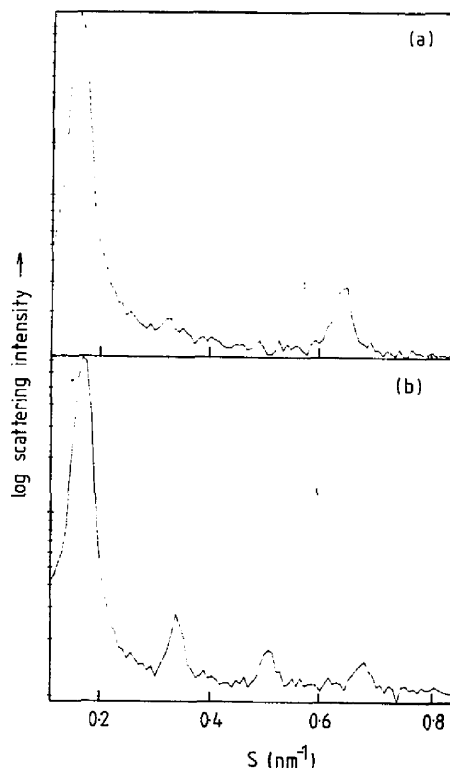


Fig. 10. Typical low-angle X-ray diffraction patterns recorded for DSPE samples in the  $L_\beta$  phase dispersed (a) in 60 wt% glycerol, (b) in 80 wt% glycerol. Measurements were made at 65°C and data collection was made over 15 s.

decrease in solvent layer thickness. It is worth noting that in the case of DPPC, the decrease in bilayer thickness is a result of lipid hydrocarbon chain interdigitation. No such interdigitation is observed in the case of DSPE dispersions.

X-ray diffraction patterns of samples containing 80 wt% and 60 wt% are presented in Fig. 10. They are typical of the patterns seen for dispersions containing less than 70 wt% and greater than 70 wt% glycerol, respectively. The only significant difference between the two sets of patterns, apart from the reduced lamellar repeat distance, is that the low-angle region of samples containing less than 70 wt% glycerol is characterised by two maxima corresponding to the first and fourth order Bragg reflections while that of samples containing 80 wt% glycerol and above is characterised by four sharp reflections of the type seen in the  $L_c$  phase (see Figs. 3a). The appearance of extra Bragg reflections in the low-angle region is consistent with an improved match between the lamellar repeat distance and the bilayer thickness favouring the idea that the reduced spacing



reflects a reduction in thickness of the glycerol-water layer separating the bilayers. Nevertheless, the possibility of a change in the tilt of the lipid chains cannot be completely excluded.

## Discussion

A diagrammatic representation of the relationship between the different phases of DSPE detected in this investigation is presented in Fig. 11. It shows many points of similarity to schemes previously reported for the short chain saturated phosphatidylethanolamine DLPE by Seddon et al. [10] and racemic mixtures of DPPE reported by Tenchov et al. [8].

As in the earlier studies, two crystalline phases are found. The close match between the wide-angle diffraction maxima of the  $L_c$  phase of DSPE and the  $B_2$  phase of DLPE [10], suggests that the hydrocarbon chains of both lipids are packed on a similar orthorhombic lattice. The lower melting point  $L_c'$  form of DSPE appears to be related to the tilted-chain  $B_1$  form of DLPE. The match between their wide angle spacings is rather poor but the ratio of the lamellar repeat distances of the  $L_c'$  and  $L_c$  forms of DSPE and the  $B_1$  and  $B_2$  forms of DLPE, 0.83 and 0.86, respectively, are very similar. This suggests that despite possible differences in chain packing, their hydrocarbon chains are tilted at similar angles to the normal to the lamellar plane.

The  $L_c$  and  $L_c'$  phases of DSPE dispersed in glycerol-free water were only observed in samples hy-

drated below their gel-to-liquid crystal transition temperature. Samples heated above this temperature relaxed into the  $L_\beta$  phase. In contrast to shorter chain phosphatidylethanolamines, there appears to be little or no tendency for DSPE to form subgel phases under these conditions. This increased difficulty in formation of the  $L_c$  and  $L_c'$  forms of the longer chain analogues of diacylphosphatidylethanolamines probably reflects the fact that the dehydration processes associated with the formation of the subgel phases are driven by changes in the headgroup arrangement of the lipids which lead to a subsequent reorganisation of the packing of the lipid chains. As the length of the chains increases, the energy required to bring about this latter re-organisation presumably increases.

The formation of lamellar subgel phases becomes increasingly facilitated as the percentage of glycerol in the dispersing medium is increased. This is reflected in shorter storage times required for the transition from the  $L_\beta$  phase to the  $L_c$  phase. It is also underlined by the fact that at higher glycerol levels the  $L_c'$  form of DSPE can be formed from the  $L_\beta$  at high temperatures (Figs. 4 and 5) and can even form from, and co-exist with, the  $H_{II}$  phase as illustrated in Fig. 7.

The most marked, and potentially the most interesting, effect of glycerol, is the stabilisation of  $H_{II}$  (and to a lesser extent of  $L_\beta$  and the two subgel phases) at the expense of  $L_\alpha$ . The increased stability of the  $H_{II}$  and  $L_\beta$  phases with respect to the  $L_\alpha$  phase, as pointed out by Koynova et al. [7] in their studies on the effects of disaccharides on the phase properties of DPPE, is consistent with an attempt by the lipid to lower the surface potential energy of the system by decreasing the extent of an energetically unfavourable interaction between the headgroups of the lipid and the surrounding medium. Similar effects are observed for proteins dissolved in glycerol/water mixtures [16–19] where addition of glycerol is found to stabilise the more compact native structure with respect to the looser thermally denatured state and hence raise the threshold temperature for thermal denaturation.

The precise nature of the interactions involved is still a matter of debate. Gekko and Morikawa [19] have demonstrated that the polyol-induced stabilisation of proteins such as chymotrypsinogen is predominantly an entropic effect probably involving solvent ordering. Collins and Washabaugh [20] have proposed a mechanism for such effects, which they consider to be a general manifestation of the Hofmeister effect. They divide the solutes that influence protein structures in aqueous solutions into kosmotropes (water-structure makers) that tend to reduce the extent of protein/water interfaces and chaotropes (water-structure breakers) that tend to increase the extent of such interfaces. They suggest that polar kosmotropes, which would include such molecules as sugars and polyols, are excluded from the interfacial

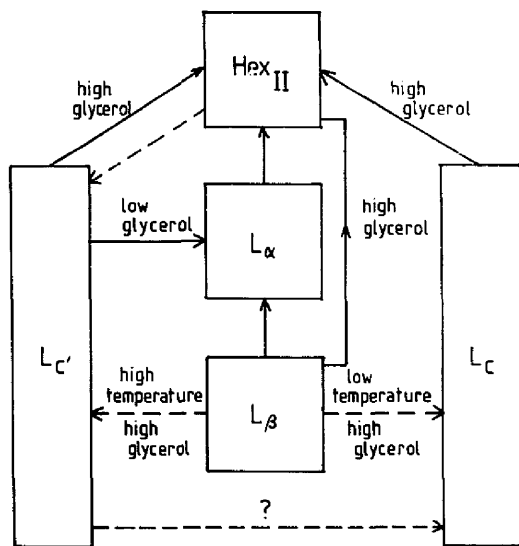


Fig. 11. Diagrammatic representation of the relationship between the different phases observed in dispersions of DSPE in excess glycerol/water mixtures.

region but tend to order the water in this region. This ordering, they argue, gives rise to an increased potential difference at the interface leading to rearrangements that tend to minimise the interfacial area.

The marked increase in stability of the  $H_{II}$  phase seen at high glycerol concentrations is consistent with its large capacity for reduction in interfacial area. This reduction, which is brought about by reducing the diameter of the water channels of the inverted micelles, is reflected in the marked decrease seen in the low-angle spacings of the  $H_{II}$  phase shown in Fig. 11. The interfacial area per molecule in the  $L_\alpha$  and  $L_\beta$  phases is given by  $4D^2/\sqrt{3}$ , where  $D$  is the wide-angle spacing [14]. The reduction in area, from  $0.449 \text{ nm}^2$  to  $0.405 \text{ nm}^2$  upon transition from the  $L_\alpha$  to the  $L_\beta$  phase is quite small. This, together with the much higher enthalpy of the transition compared to that between the  $H_{II}$  and  $L_\alpha$  phases, probably accounts for the limited change in the relative stability of the two states. The increased stability of the  $L_c$  and  $L_c'$  phases with respect to the  $L_\beta$  phase is probably of different origin. Phosphatidylethanolamines are capable of forming networks of hydrogen bonds between neighbouring headgroups [1]. The formation of such networks will certainly be favoured by low hydration but steric considerations are likely to predominate over any effects of changes in the interfacial areas.

Glycerol is a cryoprotectant and is widely used in the cryopreservation of biological cells and tissues. The molecular basis of its action is, however, still only very poorly understood. The fact that the most effective cryoprotectants are kosmotropes and as such have marked effects on the phase properties of lipids, particularly non-bilayer forming lipids, may be of importance in understanding their mode of action. The role of non-bilayer forming lipids in biological membranes is still unclear but the balance between the bilayer and non-bilayer tendencies of membrane lipids might reasonably be expected to play an important role in membrane stability [4,5]. Low temperatures favour the relaxation of non-bilayer lipids into bilayer configurations. Addition of cryoprotectants such as glycerol which tend to stabilise non-bilayer configurations at the expense of bilayer configurations would tend to restore

the balance of interactions between membrane components at low temperatures to a situation closer to that existing at physiological temperatures and hence minimise perturbations associated with low-temperature storage.

### Acknowledgements

The help and advice of Wim Bras of the Daresbury Synchrotron Facility and the support of FEBS and British Council in the form of grants are gratefully acknowledged. L.I. Tsonev was supported by a FEBS Fellowship.

### References

- 1 Hauser, H., Pascher, I., Pearson, R.H. and Sundell, S. (1981) *Biochim. Biophys. Acta* 650, 21–51.
- 2 Seddon, J.M., Ceve, G., Kaye, R.D. and Marsh, D. (1984) *Biochemistry* 23, 2634–2644.
- 3 Gordon-Kamm, W.J. and Steponkus, P.L. (1984) *Proc. Natl. Acad. Sci. USA* 81, 6373–6372.
- 4 Quinn, P.J. (1985) *Cryobiology* 22, 128–146.
- 5 Williams, W.P. (1990) *Proc. Roy. Soc. Lond. B326*, 555–570.
- 6 Bryszewska, M. and Epand, R.F. (1988) *Biochim. Biophys. Acta* 943, 485–492.
- 7 Koynova, R.D., Tenchov, B.G. and Quinn, P.J. (1989) *Biochim. Biophys. Acta* 980, 377–380.
- 8 Tenchov, B.G., Boyanov, A.I. and Koynova, R.D. (1984) *Biochemistry* 23, 3553–3558.
- 9 Tenchov, B.G., Lis, L. and Quinn, P.J. (1988) *Biochim. Biophys. Acta* 942, 305–314.
- 10 Seddon, J.M., Harlos, K. and Marsh, D. (1983) *J. Biol. Chem.* 258, 3850–3854.
- 11 Chang, H. and Epand, R.M. (1983) *Biochim. Biophys. Acta* 728, 319–324.
- 12 Mantsch, H.H., Hsi, S.C., Butler, K.W. and Cameron, D.G. (1983) *Biochim. Biophys. Acta* 728, 325–330.
- 13 Koynova, R. and Hinz, H.-J. (1990) *Chem. Phys. Lipids*, in press.
- 14 Luzzati, V. (1968) in *Biological Membranes*, Vol. 1 (Chapman, D., ed.), pp. 71–123, Academic Press, London.
- 15 McDaniel, R.V., McIntosh, T.J. and Simon, S.A. (1983) *Biochim. Biophys. Acta* 731, 97–108.
- 16 Gekko, K. and Timasheff, S.N. (1981) *Biochemistry* 20, 4667–4676.
- 17 Gekko, K. and Timasheff, S.N. (1981) *Biochemistry* 20, 4677–4686.
- 18 Gekko, K. and Morikawa, T. (1981) *J. Biochem.* 90, 39–50.
- 19 Gekko, K. and Morikawa, T. (1981) *J. Biochem.* 90, 61–77.
- 20 Collins, K.D. and Washabaugh, M.W. (1985) *Q. Rev. Biophys.* 18, 324–343.